Translational Oncology
www.transonc.com

Volume 9 Number 2 April 2016 pp. 99–107 99

HIC1 Expression Distinguishes Intestinal Carcinomas Sensitive to Chemotherapy[1,2]

Lucie Janeckova*, Michal Kolar*, Jiri Svec*,†, Lucie Lanikova*, Vendula Pospichalova*,3, Nikol Baloghova*, Martina Vojtechova*, Eva Sloncova*, Hynek Strnad* and Vladimir Korinek*,‡

*Department of Cell and Developmental Biology, Institute of Molecular Genetics, Academy of Sciences of the Czech Republic, Videnska 1083, 142 20 Prague 4, Czech Republic; †Department of Radiotherapy and Oncology, Third Faculty of Medicine, Charles University, Prague, Srobarova 50, 100 34 Prague 4, Czech Republic; ‡Division BIOCEV, Institute of Molecular Genetics, Academy of Sciences of the Czech Republic, Videnska 1083, 142 20 Prague 4, Czech Republic

Abstract

Neoplastic growth is frequently associated with genomic DNA methylation that causes transcriptional silencing of tumor suppressor genes. We used a collection of colorectal polyps and carcinomas in combination with bioinformatics analysis of large datasets to study the expression and methylation of *Hypermethylated in cancer 1* (*HIC1*), a tumor suppressor gene inactivated in many neoplasms. In premalignant stages, *HIC1* expression was decreased, and the decrease was linked to methylation of a specific region in the *HIC1* locus. However, in carcinomas, the *HIC1* expression was variable and, in some specimens, comparable to healthy tissue. Importantly, high HIC1 production distinguished a specific type of chemotherapy-responsive tumors.

Translational Oncology (2016) 9, 99–107

Introduction

Cancer is viewed as a genetic disease caused by mutations of protooncogenes and tumor suppressors. It is presumed that the first oncogenic mutation provides selective advantage to the prospective cancer cells that multiply and form the initial neoplastic lesion. Moreover, solid tumors develop over time by acquiring additional alterations that drive tumor progression (reviewed in [1]). These alterations might include extensive changes in methylation of genomic DNA that (presumably) contribute to tumorigenesis by transcriptional silencing of tumor suppressor genes (reviewed in [2]).

Adenocarcinomas affecting colon and rectum [colorectal carcinoma (CRC)] represent a major cause of morbidity and mortality in developed countries. Colorectal cancer is the third most common malignancy worldwide and the fourth most common cause of

Address all correspondence to: Vladimir Korinek, Institute of Molecular Genetics AS CR, Videnska 1083, 142 20 Prague 4, Czech Republic.
E-mail: korinek@img.cas.cz

[1] This work was supported by the Grant Agency of the Czech Republic (grant no. P305/12/2347); institutional grant (RVO 68378050); Charles University in Prague (research projects PRVOUK-Oncology P27); OPPK (CZ. 2.16/3.1.00/24024); Ministry of Education, Youth, and Sports of the Czech Republic (LO1419); and project BIOCEV (CZ.1.05/1.1.00/02.0109).

[2] **Authorship:**

Conception and design: L. Janeckova, M. Kolar, V. Korinek
Development of methodology: M. Kolar, J. Svec, L. Lanikova, V. Pospichalova, H. Strnad, V. Korinek
Acquisition of data: L. Janeckova, J. Svec, L. Lanikova, V. Pospichalova, N. Baloghova, M. Vojtechova
Analysis and interpretation of data: L. Janeckova, M. Kolar, J. Svec, L. Lanikova, V. Pospichalova, H. Strnad, V. Korinek
Writing, review, and/or revision of the manuscript: L. Janeckova, J. Svec, V. Korinek
Administrative, technical, or material support: E. Sloncova
Study supervision: V. Korinek

[3] Present address: Faculty of Science, Masaryk University, Kotlarska 2, 611 37, Brno, Czech Republic.

Received 30 November 2015; Revised 13 January 2016; Accepted 19 January 2016

1936-5233/16
http://dx.doi.org/10.1016/j.tranon.2016.01.005

cancer-related death [3]. Recently, several research consortia analyzed numerous CRCs using massive parallel sequencing and DNA microarray technologies in a comprehensive manner, yielding an unprecedented insight into the pathobiology of CRC. Consequently, the commonly accepted division of CRCs into microsatellite instable neoplasia frequently associated with increased mutation rates and CpG island methylated phenotype (CIMP), and those that display microsatellite stability but are chromosomally unstable, was recently revised (reviewed in [4]). Based on the differences in global expression profiles, six independent classification systems were proposed, dividing CRCs into three to six distinct molecular subtypes [5–10]. Very recently, reevaluation of published large-scale data resulted in subdivision of CRCs into four consensus molecular subtypes (CMSs) [11]. Importantly, because RNA expression profiles are tightly linked to the tumor phenotype, CRC molecular classification not only might improve the patient staging system but also could identify molecules or pathways for specific therapeutic interventions.

HIC1 is a tumor suppressor gene located on chromosome 17p13.3, a chromosomal region that is frequently hypermethylated, rearranged, or lost in various human cancers, including colon, lung, brain, breast, prostate, and leukemia (reviewed in [12]). The *HIC1* gene encodes an evolutionarily conserved transcriptional repressor. It is presumed that *HIC1* promoter hypermethylation leads to its silencing; however, only a limited number of reports have shown the relation between *HIC1* methylation and expression, or the results are conflicting. For example, *HIC1* promoter hypermethylation was detected in healthy brain and prostate, but because the level of the *HIC1* gene expression was not determined, no conclusion could be drawn from the observation [13–15]. Additionally, during liver carcinogenesis, the *HIC1* locus was increasingly methylated compared with the healthy tissue, precancerous lesions, and primary hepatocellular carcinomas. However, *HIC1* expression did not correlate significantly with the extent of genomic DNA methylation [16,17].

In the present study, we analyzed the *HIC1* expression pattern and locus methylation during neoplastic progression of human colorectal tumors. We used a collection of polyps and carcinomas, and, in addition, we employed large publicly available datasets that included gene expression profiling, high-throughput sequencing, and DNA methylation data of more than 970 human CRC specimens. We show that in premalignant stages, *HIC1* expression is indeed decreased, and the decrease is related to the extent of DNA methylation in a specific region in the *HIC1* locus. However, in CRC, *HIC1* expression is more variable, and some specimens display *HIC1* mRNA levels comparable to those observed in healthy tissue. Importantly, high HIC1 production distinguishes stroma-rich tumors responsive to chemotherapy.

Materials and Methods

Patients and Tissue Samples

Paired samples of normal and neoplastic tissue were obtained from 74 patients undergoing either polypectomy or surgical resection of sporadic CRC (Supplementary Table S1). The central portion of the tumor and corresponding normal colonic mucosa from the resection margin or at least 10 cm from the site of polypectomy were taken, immediately frozen, and stored in liquid nitrogen. None of the patients underwent radiotherapy or chemotherapy before the operation. The study was approved by the Ethics Committee of the Third Faculty of Medicine, Charles University, in Prague, and all patients signed the written consent to participate in the study.

Total RNA and Genomic DNA Isolation, cDNA Synthesis

Deep-frozen tissue samples were disrupted in 600 μl of lysis buffer by ceramic beads during one run of MagNA Lyser Instrument (Roche Life Sciences), and total RNA and genomic DNA were extracted using AllPrep DNA/RNA Mini kit (Qiagen) according to manufacturer's instructions. The cDNA synthesis was performed in 20-μl reaction using 1 μg of total RNA, random hexamers, and RevertAid reverse transcriptase (Thermo Scientific) according to the manufacturer's protocol.

Quantitative Reverse Transcription Polymerase Chain Reaction (qRT-PCR)

Reactions were run in triplicates using LightCycler 480 Probes Master and Universal ProbeLibrary hydrolysis probes and LightCycler 480 Instrument (Roche Life Sciences). The primer pairs and corresponding Universal ProbeLibrary probes are listed in Supplementary Table 2. Crossing point-PCR-cycle (Cp) values for each triplicate were normalized by geometric average of housekeeping genes *ubiquitin B* (*UBB*) and *TATA box binding protein* (*TBP*). Resulting values were averaged to obtain ΔCp values for biological replicates. Relative mRNA abundance (ΔCp in healthy tissue – ΔCp in neoplastic tissue) was correlated with the histological grade of tumor samples using the rank-order Spearman's (ρ) and Kendall's (τ) coefficient. Neoplastic progression was assumed as follows: hyperplasia (Hyp) < low-grade dysplasia (LGD) < high-grade dysplasia (HGD) < CRC [18].

HIC1 Immunohistochemistry

Five-micrometer sections from formalin-fixed and paraffin-embedded tissue samples were dewaxed in xylene and rehydrated. To unmask the antigen sites, the sections were immersed in a steam bath (20 minutes) in Target Retrieval Solution (Dako). Primary rabbit anti-HIC1 polyclonal antibody (ab33029, Abcam) was applied at 1:200 dilution overnight at 4°C. The primary antibody was detected using EnVision+ System (Dako), and the brown color reaction was developed with DAB (Vector Laboratories) substrate.

DNA Methylation Analysis of the HIC1 Locus in Patient Samples

Genomic DNA was isolated from deep-frozen tissue (disintegrated by MagNa Lyser System; Roche Life Sciences) using AllPrep DNA/RNA Mini kit (Qiagen). Bisulfite modification of genomic DNA (0.5 μg) from healthy and neoplastic tissue from HGD (n = 5) and CRC (n = 6) patients was performed using Imprint DNA Modification Kit (Sigma-Aldrich). Bisulfite-treated DNA was amplified using KAPA 2G Robust Hot Start ReadyMix (KapaBiosystems) and the following primers: hFHIC1: 5′-ATTATTTTTTTTAATT GGGGTAATTTTTT-3′ and hRHIC1: 5′-CCAAAACACCTAAC TAAATACTAAAACTTC-3′. The purified products were subcloned into the pGEM-T-Easy vector (Promega), and at least eight positive clones were sequenced. Sequencing data for CpG methylation were analyzed using the online quantification tool for methylation analysis (QUMA) (Laboratory for Mammalian Epigenetic Studies, Center for Developmental Biology, RIKEN).

Public CRC Datasets and Statistical Analysis

The GSE33113 [6] dataset was retrieved from ArrayExpress [19] (accession E-GEOD-33113); the GSE13294 [20], GSE14333 [21], and GSE62080 [22] datasets were retrieved from the Gene

Expression Omnibus [23] repository. The Cancer Genome Atlas (TCGA) data were accessed from the TCGA repository (Broad Institute, Massachusetts Institute of Technology, USA) on April 13, 2015. The expression, methylation, and mutational analyses are described in Supplementary material. All computations and statistical tests were performed in the R environment [24].

Results and Discussion

Region-Specific Methylation of the HIC1 locus in CRC

To determine changes in the *HIC1* expression levels during neoplastic progression, we analyzed total RNA isolated from the matched healthy colonic mucosa and neoplastic tissue obtained from 74 patients. In adenomas, we observed significant decreases in *HIC1* expression in polyps with low- and high-grade dysplasia when compared with healthy or hyperplastic tissue. *HIC1* expression in CRCs was more heterogeneous, with median positioned between healthy/hyperplastic and dysplastic samples (Figure 1*A*). To explore the relationship between *HIC1* expression and the methylation status of CRCs, we interrogated the relevant dataset recently available from the TCGA consortium (https://tcga-data.nci.nih.gov/tcga/; 277 specimens in total; the dataset was designated TCGA 450K; see Supplementary Materials and Methods for details). Unsupervised clustering of DNA methylation profiles identified four subgroups of tumors. Two of the subgroups contained CRCs with elevated methylation and were classified according to previously published nomenclature [25,26] as CIMP-high and CIMP-low. The two non-CIMP clusters were designated non–CIMP I and non–CIMP II. In addition, we employed TCGA gene expression data and determined (relative) *HIC1* mRNA expression levels in each CRC. Samples that (according to *HIC1* expression) fell into the first and last decile were defined as "HIC1-high" and "HIC1-low," respectively. The majority of the HIC1-high samples were distributed among the CIMP-low, non–CIMP I, and non–CIMP II subgroups. Surprisingly, we did not observe clear correlation between the CRC CIMP status and *HIC1* expression. In fact, one HIC1-high sample was found in the CIMP-high subgroup. Moreover, the HIC1-low samples were "scattered" among all four subgroups (Figure 1*B*). To analyze the methylation rate of *HIC1*, we evaluated the methylation status of the *HIC1* locus. A substantial portion of mammalian genes contain the so-called CpG island, a promoter region rich in CpG nucleotides that are frequently methylated (reviewed in [27]). However, several studies have shown that most of the methylation changes in cancer DNA do not occur in the promoter CpG islands but in the regions located up to 2 kbp apart or even more distant. Importantly, the methylation status of these CpG island "shores" or "shelves" is strongly related to gene expression [28–30]. Up to six different *HIC1* isoforms were detected in various tissues with predominance of *HIC1a* mRNA. These isoforms are produced by differential splicing or usage of three alternative promoters (reviewed in [31]). Accordingly, two CpG islands and adjacent shores and shelves (including all three promoters) were assigned to the locus (Figure 2*A*). Using the TCGA 450K dataset, we retrieved information about methylation of 62 DNA probes covering a large portion of the *HIC1* gene. Methylation probes with median of the methylated fraction equal to or greater than 50% (beta value ≥ 0.5) in the CIMP-high subgroup and median of the methylated fraction equal to or lesser than 20% (beta value ≤ 0.2) in both non-CIMP subgroups were considered as CIMP status-related (Supplementary Figure S1). Additionally, methylation probes whose methylation correlated with decreasing *HIC1* expression (LM-fit coefficient ≤ −1) were identified as expression-related (Supplementary Figure S2). Interestingly, we identified 31 CIPM-related methylation probes that were located exclusively in CpG island 1. In contrast, all seven probes related to *HIC1* expression were found in CpG island/shore 2. Subsequently, we confirmed the observation by testing methylation of genomic DNA isolated from our collection of healthy and neoplastic colorectal tissue. The cytosine methylation analysis was performed in the shore region upstream to CpG island 2 because the very high CG content of the island itself precluded any unbiased evaluation (Figure 3*A*). Analysis of the sequence containing 10 CpG

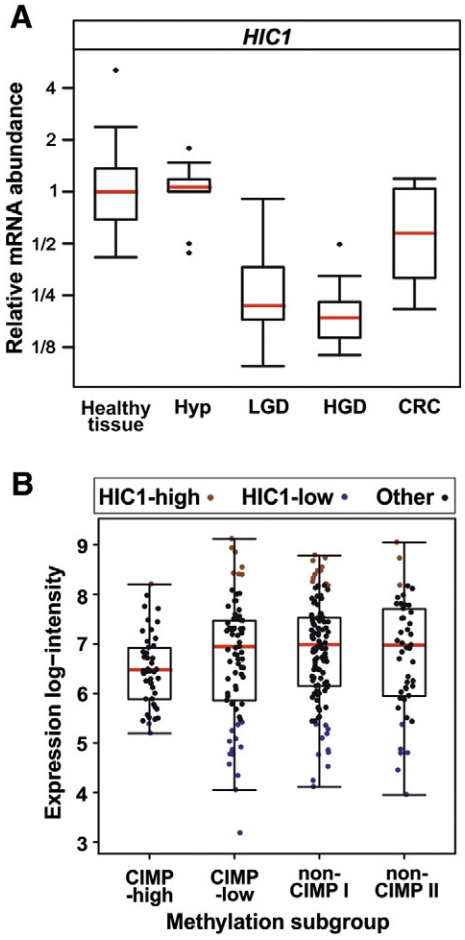

Figure 1. Analysis of *HIC1* expression in colorectal neoplasia. (A) *HIC1* expression changes during tumor progression. qRT-PCR analysis of the *HIC1* mRNA levels in healthy tissue, hyperplastic adenomas (Hyp; $n = 9$), adenomas displaying low-grade (LGD; $n = 24$) or high-grade (HGD; $n = 25$) dysplasia, and CRC ($n = 12$). The boxed areas correspond to the second and third quartiles; the median of ΔCp values for each category is indicated as the red line. The relation between the *HIC1* expression profile and neoplasia progression is significant, as evidenced by the Spearman's ($\rho = -0.67$) and Kendall's ($\tau = -0.51$) coefficient values. (B) *HIC1* expression in CRC subgroups clustered according to the DNA methylation profiles. HIC1-high and HIC1-low samples are indicated by brown or blue dots, respectively. Black dots indicate the other specimens. The red lines correspond to the median values; log2-expression intensity, binary logarithm of expression intensity (additional details are given in Supplementary Methods).

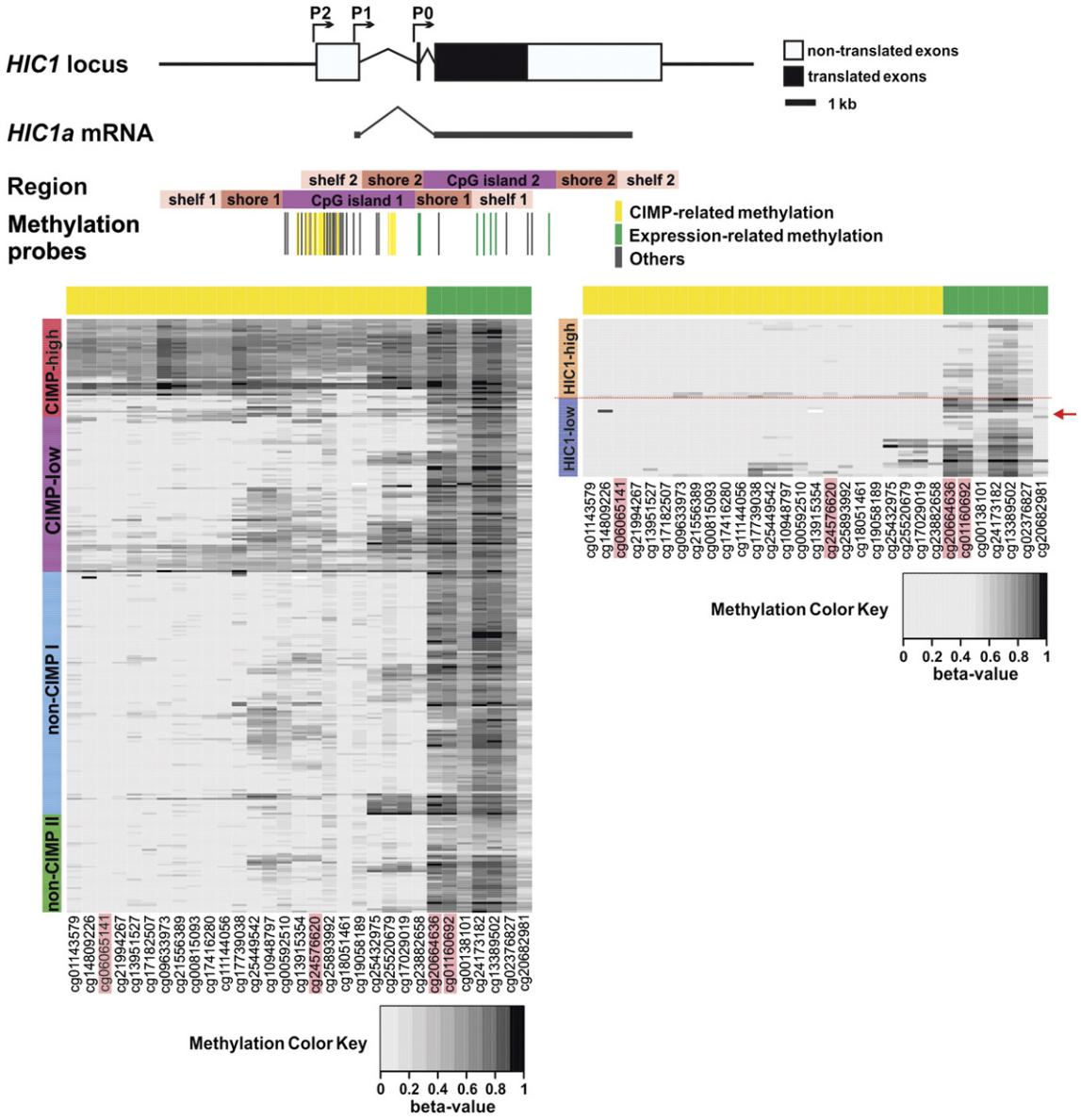

Figure 2. Identification of the CIMP-related and gene expression–related *HIC1* methylation sites. Top, the *HIC1* gene exon-intron structure indicating the position of the major *HIC1a* transcript driven from the P1 promoter; the position of two alternative promoters P2 and P0 is also shown. A color-based classification of two CpG islands and other elements is indicated under the schemes; methylation probes covering the *HIC1* locus are indicated as horizontal bars. The bottom panels depict the *HIC1* methylation status in 277 CRC cases present in the TCGA 450K dataset. In the left panel, the specimens were grouped according to the CIMP status of tumor DNA; each specimen is represented by a horizontal bar. The right panel shows the *HIC1* methylation status in CRCs classified as HIC1-high or HIC1-low; the sample with the *HIC1* locus deletion is indicated by red arrow. The extent of methylation of CIMP-related (yellow) and expression-related probes (green) is shown as the gray-shaded heatmap of beta values (unmethylated: white; completely methylated: black); notice the different "slope" of beta values between the left and right panel. Probes are listed vertically with their identification code in a successive order according to their target sequence coordinates (the 5′ gene end is shown on the left). The CRC methylation profile of four probes boxed in pink is shown in Supplementary Figure S1. The correlation between *HIC1* expression and the methylation profile of these four probes is given in Supplementary Figure S2.

doublets located in (or surrounding) the second *HIC1* exon revealed increased methylation in DNA isolated from HGD specimens when compared with DNA obtained from the matched healthy mucosa (Figure 3*B*). Additionally, in CRCs, we observed a clear difference in the methylation status between the HIC1-high and HIC1-low specimens (Figure 3*C*). We noted a complete absence of methylation in the expression-related region in one sample from the HIC1-low group (red arrow in Figure 2). However, subsequent copy-number variation analysis revealed deletion of the chromosomal region harboring the *HIC1* locus in this particular sample, thus explaining the lack of the signal. *HIC1* transcription is activated by p53 [32,33], and we therefore analyzed *TP53* gene mutations in TCGA 450K CRCs. However, we did not find any significant differences in the *TP53* status in HIC1-high [3 specimens harboring wild-type (wt) and 21 specimens mutant *TP53*] when compared with HIC1-low samples (5 wt vs 15 mutant specimens). Nevertheless, this does not

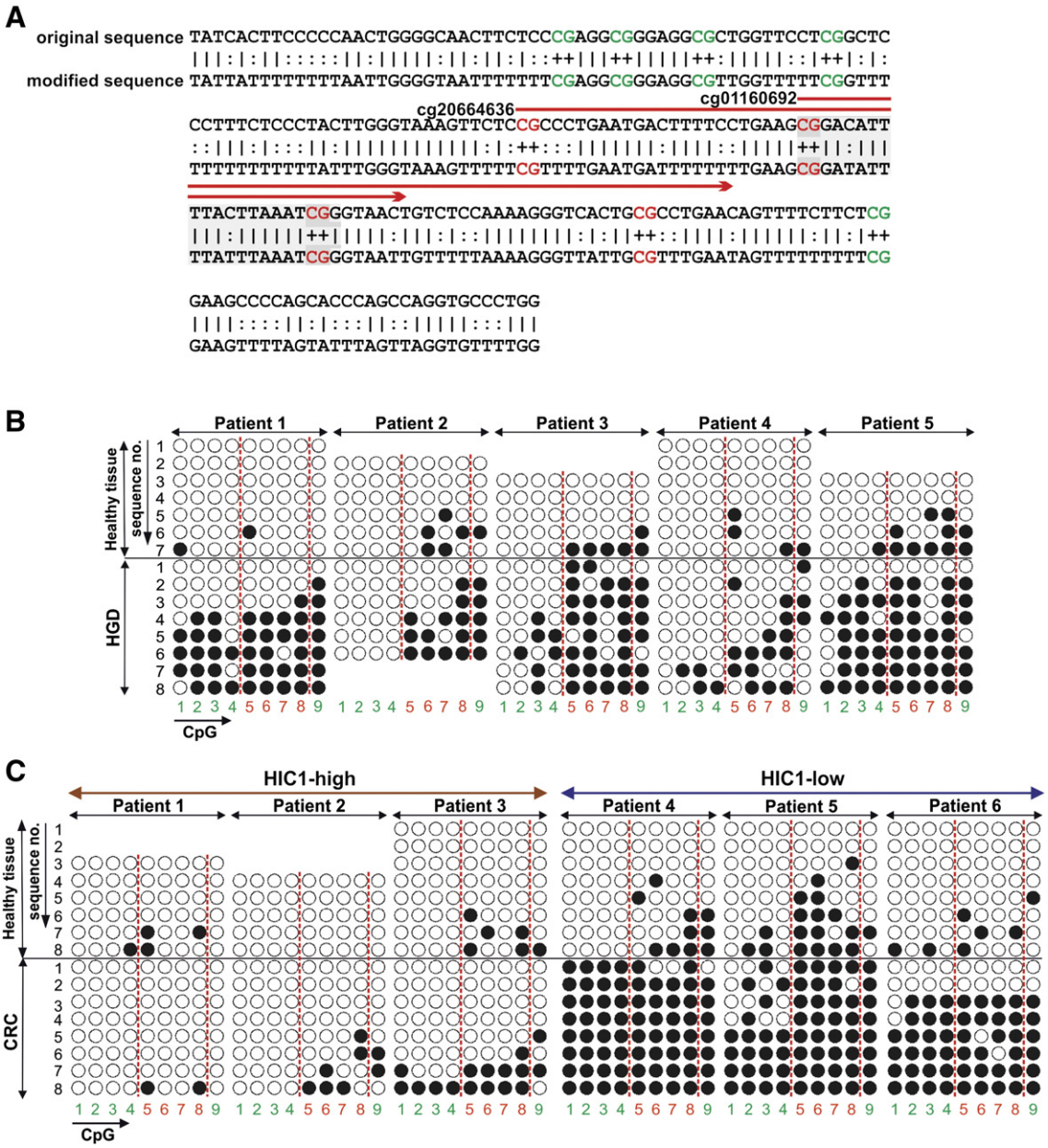

Figure 3. Cytosine methylation analysis of the *HIC1* locus. (A) Original and bisulfite-modified DNA sequence containing the second (alternative) *HIC1* exon (boxed in grey). Methylation probes included in the region are indicated by red arrows above the sequences. CpG dinucleotides located in the sequence covered by the probes are in red; other CpG dinucleotides are in green. (B) Methylation of genomic DNA isolated from colorectal polyps displaying HGD and genomic DNA obtained from matched healthy tissue. Open circles mark unmethylated CpG dinucleotides, whereas closed circles indicate methylated CpGs; the numbering and color code of CpGs correspond to their positions in the analyzed genomic DNA as indicated in (A). (C) Cytosine methylation analysis of genomic DNA isolated from three HIC1-high and three HIC1-low CRCs.

exclude that a transcriptional mechanism other than p53-dependent might—next to the epigenetic modifications—contribute to *HIC1* expression.

High HIC1 Expression in CRCs Responsive to Chemotherapy

Next, we asked whether the *HIC1* expression level is connected with some specific pathological CRC features using information contained in the TCGA 450K and additional three datasets TCGA 27K [34], GSE13294 [20], and GSE14333 [21] (the latter two datasets were processed together). Rather surprisingly, that is, considering the tumor suppressive role of HIC1, patients with HIC1-high CRCs displayed lower survival than patients with HIC1-low CRCs, although a significant difference was reached in the TCGA 27K dataset only (Figure 4*A*). Interestingly, an opposite phenomenon, that is, association of higher *HIC1* expression with better clinical outcome, was observed in breast [35] or lung cancer [36]. The discrepancy might be attributed to the fact that more progressed malignancies prevailed among HIC1-high CRCs (Supplementary Figure S3). On the other hand, according to cancer-treatment related information retrieved from the GSE13294, GSE14333, and GSE62080 [22] datasets, patients from the HIC1-high group responded significantly better to FOLFIRI treatment than

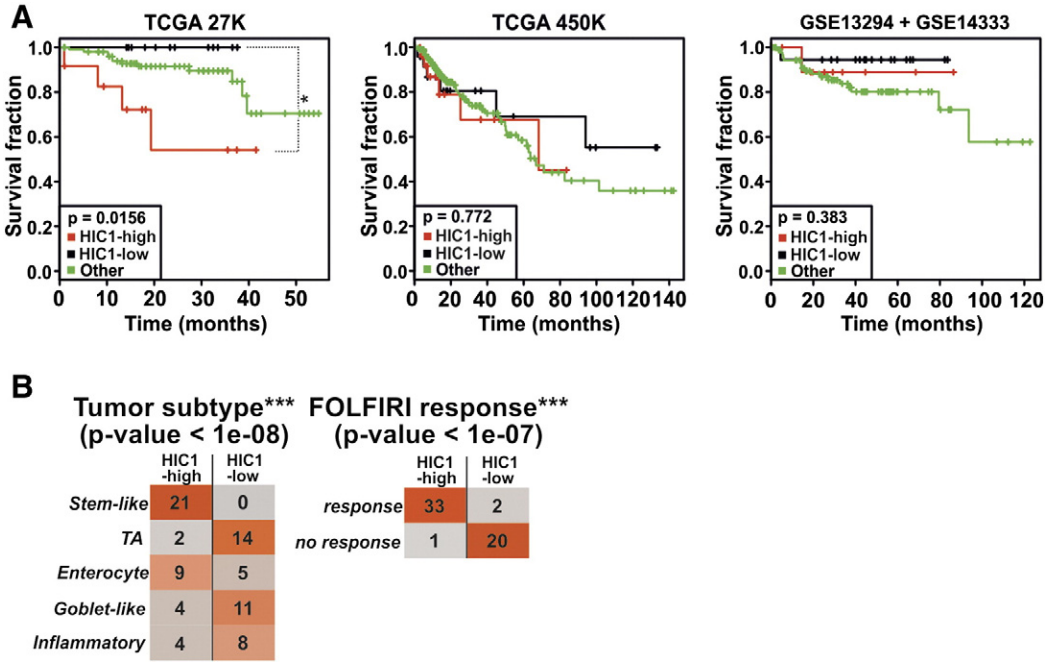

Figure 4. HIC1-high CRCs are responsive to FOLFIRI treatment. (A) Kaplan-Meier plots of patient survival for indicated datasets. (B) Assignment of HIC1-high/low CRCs from the GSE13294 and GSE14333 datasets according to CRC subtype clustering and FOLFIRI response as described in reference [9]. *$P < .05$; ***$P < .001$ (Student's t test).

patients from the HIC1-low group (Figure 4*B* and Supplementary Figure S4). Of note, FOLFIRI, that is, combination of folinic acid (FOL/leucovorin), 5-fluorouracil, and topoisomerase inhibitor irinotecan (IRI), is used as the first-line therapy to improve maximal survival of patients with metastatic CRCs [37]. Based on expression profiles, we clustered CRCs from these datasets to stem-like, enterocyte, transit-amplifying, goblet-like, and inflammatory subtypes [9]. Interestingly, 53% of HIC1-high tumors (n = 21) were assigned to the stem-like tumors that were associated with clinical benefits of FOLFIRI treatment (Figure 4*B*).

The HIC1-High CRC Group and CMS4 Cancer Subtype Relationship

Finally, we obtained another CRC dataset, GSE33113 [6], and employed expression data representing 971 CRCs in total to identify the expression signature that distinguishes HIC1-high from HIC1-low CRC samples. Unbiased hierarchical clustering revealed 298 genes whose expression differed significantly between HIC1-high and HIC1-low tumors (Figure 5*A*, Supplementary Table S3). All these genes except *C2 calcium-dependent domain containing 4A* (*C2CD4A*) were upregulated in HIC1-high samples. This indicated—considering the transcriptionally repressive function of HIC1—that the selected genes are not directly regulated by HIC1. Indeed, none of the previously identified HIC1-repressed genes [38–48] was present among the genes. Nevertheless, qRT-PCR analysis of *C2CD4A* and five other genes highly upregulated in HIC1-high samples using eight CRC samples from our experimental collection (four CRCs were selected as HIC1-high, additional four as HIC1-low) supported the observation made "*in silico*" (Figure 5*B*). Additionally, the obtained gene set was evaluated using the Enricher gene library online tool (http://amp.pharm.mssm.edu/Enrichr/) [49]. We performed gene set enrichment analysis to assign the "Gene Ontology Biological Processes" (GO Biological Processes), Kyoto Encyclopedia of Genes and Genomes pathways, and "GO Cellular Components" categories to the signature genes. The analysis revealed that the majority of identified genes encode secreted proteins that are involved in extracellular matrix organization and focal adhesion (Supplementary Figure S5, Supplementary Table S4).

Subsequently, we stratified individual CRC samples into four recently defined CMSs [11]. Strikingly, all HIC1-high samples were present in the CMS4 subtype (Figure 5*C*) that is characterized by stromal invasion, activation of transforming growth factor β (TGF-β) signaling, and extracellular matrix remodeling and complement-mediated inflammatory pathways. Indeed, genes encoding the TGF-β1 ligand and complement components were present among upregulated genes in HIC1-high tumors (Supplementary Table S4). Very recently, Calon and colleagues described an aggressive stem-like/mesenchymal CRC subtype with poor prognosis. Strikingly, the expression profile of this particular CRC subtype is related to the gene expression program induced by TGF-β in tumor stromal cells [50]. To this end, we compared genes upregulated in HIC1-high tumors with the TGF-β response gene signatures in different types of stromal cells. We found significant overlaps of gene profiles by TGF-β–activated normal colonic fibroblasts (including *HIC1* that was among the TGF-β–activated genes), macrophages, and endothelial cells (Supplementary Table S5). This would suggest that (in some CRCs) *HIC1* is expressed in stromal rather than in epithelial tumor cells. However, immunohistochemical staining clearly revealed HIC1-positive nuclei (and the cytoplasm) in the healthy colonic epithelium and in tumor cells in HIC1-high CRC samples. Additionally, HIC1 positivity was detected in the nuclei of cells present in the *lamina propria* and in tumor stroma of both HIC1-high and HIC1-low samples (Figure 5*D*).

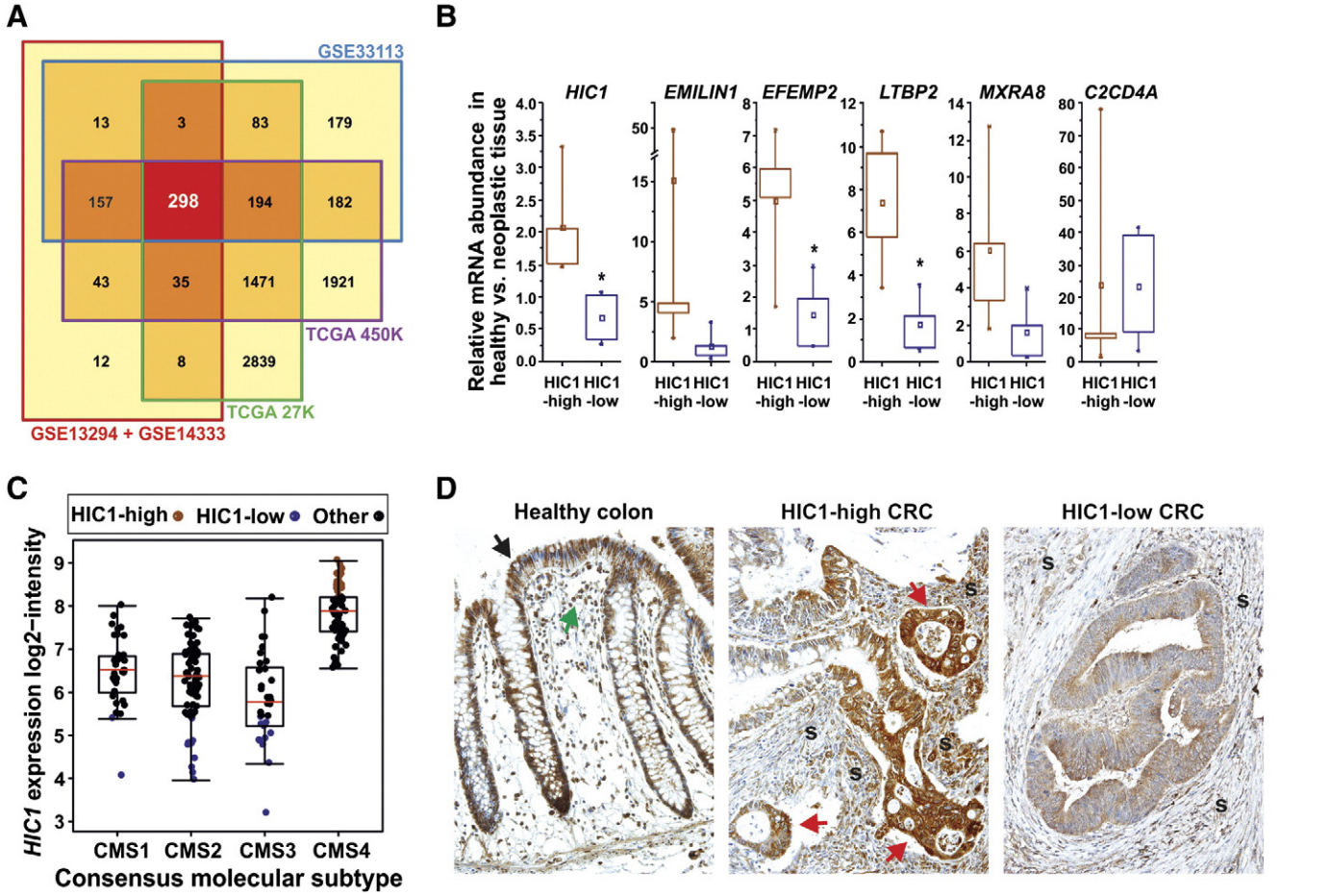

Figure 5. All HIC1-high tumors are present in the CMS4 CRC subtype. (A) Venn diagram indicating numbers of genes differentially expressed in HIC1-high versus HIC1-low CRCs in the indicated datasets; significance criterion: q value < 0.05; absolute value of log2 of relative expression intensity (|log2 FC|) ≥ 1 for at least one of the gene-specific probes. (B) qRT-PCR analysis of genes differentially expressed in HIC1-high (n = 4) and HIC1-low (n = 4) CRCs. HIC1-high CRC upregulated genes: *elastin microfibril interfacer 1* (*EMILIN1*), *EGF containing fibulin-like extracellular matrix protein 2* (*EFEMP2*), *latent transforming growth factor beta binding protein 2* (*LTBP2*), *matrix-remodeling associated 8* (*MXRA8*); downregulated gene: *C2CD4A*. (C) Assignment of HIC1-high, HIC1-low, and "other" specimens from the TCGA 450K dataset to the CMS groups. (D) Representative microscopy images of HIC1 protein immunohistochemical detection using DAB staining (brownish precipitate). HIC1-positive epithelial and *lamina propria* cells in the healthy colon are indicated by black and green arrows, respectively. Red arrows point at HIC1-positive epithelial cancer cells in HIC1-high CRC. Anti-HIC1 staining was also observed in the stroma (s) of both HIC1-high and HIC1-low CRC tumors. The specimens were counterstained with hematoxylin (blue nuclei). Magnification: 200×.

Cancer-associated fibroblasts are the main source of TGF-β ligand in colorectal tumors [51]. Interestingly, Chen and colleagues reported that the *HIC1* gene was induced in primary lung cancer cells cocultured with cancer-associated fibroblasts [52]. In addition, exposure of non–small cell lung cancer cells to TGF-β also led to the increased *HIC1* mRNA levels [53]. Of note, both observations were obtained upon interrogation of the corresponding datasets deposited by the authors to the ArrayExpress repository at https://www.ebi.ac.uk/arrayexpress. Finally, Briones and colleagues found that the repression of fibroblast growth factor-binding protein 1 by TGF-β signaling depends on HIC1 [40]. These data suggest a functional relationship between cancer and stromal (i.e., TGF-β-producing) cells in *HIC1*-expressing CRCs. In contrast, Calon and colleagues reported that because of the mutations in genes encoding components of TGF-β signaling, many epithelial cancer cells are not responsive to the TGF-β cues [50]. To solve this possible discrepancy, we used exome sequence data from the TCGA 450K dataset to identify mutations in the TGFβ1 branch of TGF-β signaling in the CMS4 group of tumors. We found frequent missense mutations in the *SMAD4* gene encoding the common cytoplasmic/nuclear mediator of the signaling. However, these mutations were equally distributed among HIC1-high and "other" tumors. Nonetheless, none of the identified inactivating mutations [affecting genes encoding TGFBR1, SMAD2, and SMAD4] was found in HIC1-high samples. Interestingly, in 17 of 50 CRCs, we did not detect any mutations in the TGFβ1-dependent branch of the pathway (Supplementary Figure S6). This might imply that epithelial cancer cells in (some) stroma-rich CRCs retained TGF-β responsiveness. How is *HIC1* (re)expression in CRC regulated? What is the function of the protein in progressed CRC, and why is a portion of the HIC1 protein in tumor cells cytoplasmic? These intriguing questions remain to be elucidated. However, our results clearly indicate that *HIC1* expression defines a group of CRCs sensitive to FOLFIRI treatment. The study also documents how high-throughput approaches started

to shape current biomedical and molecular biology research. Clinically relevant data can be produced by "data mining" of large publicly available datasets that are complemented by experiments using a relatively small collection of clinical samples.

Conclusions

(1) Region-specific methylation dictates the *HIC1* expression levels in intestinal cancer.
(2) High HIC1 production distinguishes stroma-rich carcinomas responsive to chemotherapy.

Conflict of Interest

There are no conflicts of interest to disclose.

Acknowledgements

We thank S. Takacova for critically reading the manuscript and K. Vadinska for histology. We are deeply grateful to all specimen donors and research groups that have made the data publicly available. This work was supported by the Grant Agency of the Czech Republic (grant no. P305/12/2347); institutional grant (RVO 68378050); Charles University in Prague (research projects PRVOUK-Oncology P27); OPPK (CZ. 2.16/3.1.00/24024); Ministry of Education, Youth, and Sports of the Czech Republic (LO1419); and project BIOCEV (CZ.1.05/1.1.00/02.0109).

Appendix A. Supplementary data

Supplementary data to this article can be found online at http://dx.doi.org/10.1016/j.tranon.2016.01.005.

References

[1] Kinzler KW and Vogelstein B (1996). Lessons from hereditary colorectal cancer. *Cell* **87**, 159–170.
[2] Jones PA and Baylin SB (2002). The fundamental role of epigenetic events in cancer. *Nat Rev Genet* **3**, 415–428.
[3] Siegel R, Desantis C, and Jemal A (2014). Colorectal cancer statistics, 2014. *CA Cancer J Clin* **64**, 104–117.
[4] Van Schaeybroeck S, Allen WL, Turkington RC, and Johnston PG (2011). Implementing prognostic and predictive biomarkers in CRC clinical trials. *Nat Rev Clin Oncol* **8**, 222–232.
[5] Budinska E, et al (2013). Gene expression patterns unveil a new level of molecular heterogeneity in colorectal cancer. *J Pathol* **231**, 63–76.
[6] De Sousa EMF, et al (2013). Poor-prognosis colon cancer is defined by a molecularly distinct subtype and develops from serrated precursor lesions. *Nat Med* **19**, 614–618.
[7] Marisa L, et al (2013). Gene expression classification of colon cancer into molecular subtypes: characterization, validation, and prognostic value. *PLoS Med* **10**e1001453.
[8] Roepman P, et al (2014). Colorectal cancer intrinsic subtypes predict chemotherapy benefit, deficient mismatch repair and epithelial-to-mesenchymal transition. *Int J Cancer* **134**, 552–562.
[9] Sadanandam A, et al (2013). A colorectal cancer classification system that associates cellular phenotype and responses to therapy. *Nat Med* **19**, 619–625.
[10] Schlicker A, et al (2012). Subtypes of primary colorectal tumors correlate with response to targeted treatment in colorectal cell lines. *BMC Med Genomics* **5**, 66.
[11] Guinney J, et al (2015). The consensus molecular subtypes of colorectal cancer. *Nat Med* **21**, 1350–1356.
[12] Fleuriel C, Touka M, Boulay G, Guerardel C, Rood BR, and Leprince D (2009). HIC1 (hypermethylated in cancer 1) epigenetic silencing in tumors. *Int J Biochem Cell Biol* **41**, 26–33.
[13] Morton Jr RA, Watkins JJ, Bova GS, Wales MM, Baylin SB, and Isaacs WB (1996). Hypermethylation of chromosome 17P locus D17S5 in human prostate tissue. *J Urol* **156**, 512–516.
[14] Rood BR, Zhang H, Weitman DM, and Cogen PH (2002). Hypermethylation of HIC-1 and 17p allelic loss in medulloblastoma. *Cancer Res* **62**, 3794–3797.
[15] Uhlmann K, et al (2003). Distinct methylation profiles of glioma subtypes. *Int J Cancer* **106**, 52–59.
[16] Kanai Y, Hui AM, Sun L, Ushijima S, Sakamoto M, Tsuda H, and Hirohashi S (1999). DNA hypermethylation at the D17S5 locus and reduced HIC-1 mRNA expression are associated with hepatocarcinogenesis. *Hepatology* **29**, 703–709.
[17] Nishida N, Nagasaka T, Nishimura T, Ikai I, Boland CR, and Goel A (2008). Aberrant methylation of multiple tumor suppressor genes in aging liver, chronic hepatitis, and hepatocellular carcinoma. *Hepatology* **47**, 908–918.
[18] Schlemper RJ, et al (2000). The Vienna classification of gastrointestinal epithelial neoplasia. *Gut* **47**, 251–255.
[19] Kolesnikov N, et al (2015). ArrayExpress update—simplifying data submissions. *Nucleic Acids Res* **43**, D1113–D1116.
[20] Jorissen RN, et al (2008). DNA copy-number alterations underlie gene expression differences between microsatellite stable and unstable colorectal cancers. *Clin Cancer Res* **14**, 8061–8069.
[21] Jorissen RN, et al (2009). Metastasis-associated gene expression changes predict poor outcomes in patients with Dukes Stage B and C colorectal cancer. *Clin Cancer Res* **15**, 7642–7651.
[22] Del Rio M, et al (2007). Gene expression signature in advanced colorectal cancer patients select drugs and response for the use of leucovorin, fluorouracil, and irinotecan. *J Clin Oncol* **25**, 773–780.
[23] Barrett T, et al (2013). NCBI GEO: archive for functional genomics data sets—update. *Nucleic Acids Res* **41**, D991–D995.
[24] Team RC (2014). R: A Language and Environment for Statistical Computing. . 2012 ed.Vienna, Austria: R Foundation for Statistical Computing3-900051-07-0; 2014 .
[25] Hinoue T, et al (2012). Genome-scale analysis of aberrant DNA methylation in colorectal cancer. *Genome Res* **22**, 271–282.
[26] Kawasaki T, Ohnishi M, Nosho K, Suemoto Y, Kirkner GJ, Meyerhardt JA, Fuchs CS, and Ogino S (2008). CpG island methylator phenotype-low (CIMP-low) colorectal cancer shows not only few methylated CIMP-high-specific CpG islands, but also low-level methylation at individual loci. *Mod Pathol* **21**, 245–255.
[27] Jones PA (2012). Functions of DNA methylation: islands, start sites, gene bodies and beyond. *Nat Rev Genet* **13**, 484–492.
[28] Berman BP, et al (2012). Regions of focal DNA hypermethylation and long-range hypomethylation in colorectal cancer coincide with nuclear lamina-associated domains. *Nat Genet* **44**, 40–46.
[29] Bibikova M, et al (2011). High density DNA methylation array with single CpG site resolution. *Genomics* **98**, 288–295.
[30] Irizarry RA, et al (2009). The human colon cancer methylome shows similar hypo- and hypermethylation at conserved tissue-specific CpG island shores. *Nat Genet* **41**, 178–186.
[31] Jenal M, Britschgi C, Fey MF, and Tschan MP (2010). Inactivation of the hypermethylated in cancer 1 tumour suppressor—not just a question of promoter hypermethylation? *Swiss Med Wkly* **140**, w13106.
[32] Mondal AM, Chinnadurai S, Datta K, Chauhan SS, Sinha S, and Chattopadhyay P (2006). Identification and functional characterization of a novel unspliced transcript variant of HIC-1 in human cancer cells exposed to adverse growth conditions. *Cancer Res* **66**, 10466–10477.
[33] Wales MM, Biel MA, el Deiry W, Nelkin BD, Issa JP, Cavenee WK, Kuerbitz SJ, and Baylin SB (1995). p53 activates expression of HIC-1, a new candidate tumour suppressor gene on 17p13.3. *Nat Med* **1**, 570–577.
[34] Cancer Genome Atlas Research, N., et al (2013). The Cancer Genome Atlas Pan-Cancer analysis project. *Nat Genet* **45**, 1113–1120.
[35] Nicoll G, Crichton DN, McDowell HE, Kernohan N, Hupp TR, and Thompson AM (2001). Expression of the hypermethylated in cancer gene (HIC-1) is associated with good outcome in human breast cancer. *Br J Cancer* **85**, 1878–1882.
[36] Hayashi M, et al (2001). Reduced HIC-1 gene expression in non-small cell lung cancer and its clinical significance. *Anticancer Res* **21**, 535–540.
[37] Grothey A, Sargent D, Goldberg RM, and Schmoll HJ (2004). Survival of patients with advanced colorectal cancer improves with the availability of fluorouracil-leucovorin, irinotecan, and oxaliplatin in the course of treatment. *J Clin Oncol* **22**, 1209–1214.
[38] Boulay G, Malaquin N, Loison I, Foveau B, Van Rechem C, Rood BR, Pourtier A, and Leprince D (2012). Loss of hypermethylated in cancer 1 (HIC1) in breast cancer cells contributes to stress-induced migration and invasion through beta-2 adrenergic receptor (ADRB2) misregulation. *J Biol Chem* **287**, 5379–5389.

[39] Briggs KJ, Corcoran-Schwartz IM, Zhang W, Harcke T, Devereux WL, Baylin SB, Eberhart CG, and Watkins DN (2008). Cooperation between the Hic1 and Ptch1 tumor suppressors in medulloblastoma. *Genes Dev* **22**, 770–785.

[40] Briones VR, Chen S, Riegel AT, and Lechleider RJ (2006). Mechanism of fibroblast growth factor-binding protein 1 repression by TGF-beta. *Biochem Biophys Res Commun* **345**, 595–601.

[41] Dehennaut V, Loison I, Boulay G, Van Rechem C, and Leprince D (2013). Identification of p21 (CIP1/WAF1) as a direct target gene of HIC1 (hypermethylated in cancer 1). *Biochem Biophys Res Commun* **430**, 49–53.

[42] Foveau B, Boulay G, Pinte S, Van Rechem C, Rood BR, and Leprince D (2012). The receptor tyrosine kinase EphA2 is a direct target gene of hypermethylated in cancer 1 (HIC1). *J Biol Chem* **287**, 5366–5378.

[43] Chen WY, Wang DH, Yen RC, Luo J, Gu W, and Baylin SB (2005). Tumor suppressor HIC1 directly regulates SIRT1 to modulate p53-dependent DNA-damage responses. *Cell* **123**, 437–448.

[44] Janeckova L, et al (2015). HIC1 tumor suppressor loss potentiates TLR2/NF-kappaB signaling and promotes tissue damage-associated tumorigenesis. *Mol Cancer Res* **13**, 1139–1148.

[45] Van Rechem C, Boulay G, Pinte S, Stankovic-Valentin N, Guerardel C, and Leprince D (2010). Differential regulation of HIC1 target genes by CtBP and NuRD, via an acetylation/SUMOylation switch, in quiescent versus proliferating cells. *Mol Cell Biol* **30**, 4045–4059.

[46] Van Rechem C, et al (2009). Scavenger chemokine (CXC motif) receptor 7 (CXCR7) is a direct target gene of HIC1 (hypermethylated in cancer 1). *J Biol Chem* **284**, 20927–20935.

[47] Vilgelm AE, Hong SM, Washington MK, Wei J, Chen H, El-Rifai W, and Zaika A (2010). Characterization of DeltaNp73 expression and regulation in gastric and esophageal tumors. *Oncogene* **29**, 5861–5868.

[48] Zhang W, et al (2010). A potential tumor suppressor role for Hic1 in breast cancer through transcriptional repression of ephrin-A1. *Oncogene* **29**, 2467–2476.

[49] Chen EY, Tan CM, Kou Y, Duan Q, Wang Z, Meirelles GV, Clark NR, and Ma'ayan A (2013). Enrichr: interactive and collaborative HTML5 gene list enrichment analysis tool. *BMC Bioinformatics* **14**, 128.

[50] Calon A, et al (2015). Stromal gene expression defines poor-prognosis subtypes in colorectal cancer. *Nat Genet* **47**, 320–329.

[51] Calon A, et al (2012). Dependency of colorectal cancer on a TGF-beta-driven program in stromal cells for metastasis initiation. *Cancer Cell* **22**, 571–584.

[52] Chen WJ, et al (2014). Cancer-associated fibroblasts regulate the plasticity of lung cancer stemness via paracrine signalling. *Nat Commun* **5**, 3472.

[53] Sun Y, et al (2014). Metabolic and transcriptional profiling reveals pyruvate dehydrogenase kinase 4 as a mediator of epithelial-mesenchymal transition and drug resistance in tumor cells. *Cancer Metab* **2**, 20.